HHS Public Access

Author manuscript

Placenta. Author manuscript; available in PMC 2021 June 01.

Published in final edited form as:

Placenta. 2020 June ; 95: 18–25. doi:10.1016/j.placenta.2020.04.007.

Deletion of Atypical Chemokine Receptor 3 (ACKR3) increases immune cells at the fetal-maternal interface

Kelsey E. Quinn[a], **Brooke C. Matson**[a], **Kathleen M. Caron**[a,b,c]

[a]Department of Cell Biology and Physiology, 111 Mason Farm Road, 6312B Medical Biomolecular Research Building, CB# 7545, Chapel Hill, North Carolina 27599, USA

[b]Department of Genetics, 111 Mason Farm Road, 6312B Medical Biomolecular Research Building, CB# 7545, Chapel Hill, North Carolina 27599, USA

[C]Lineberger Comprehensive Cancer Center, 111 Mason Farm Road, 6312B Medical Biomolecular Research Building, CB# 7545, Chapel Hill, North Carolina 27599, USA

Abstract

Establishment of immune cell populations and adaptations in immune cells are critical aspects during pregnancy that lead to protection of the semi-allogenic fetus. Appropriate immune cell activation and trophoblast migration are regulated in part by chemokines, the availability of which can be fine-tuned by decoy receptors. Atypical chemokine receptor 3 (ACKR3), previously named C-X-C chemokine receptor 7 (CXCR7), is a chemokine decoy receptor expressed in placenta, but little is known about how this receptor affects placental development. In this study, we investigated the phenotypic characteristics of placentas from *Ackr3*$^{-/-}$ embryos to determine how *Ackr3* contributes to early placentation. In placentas from *Ackr3*$^{-/-}$ embryos, we observed an increase in decidual compaction and in the size of the uterine natural killer cell population. *Ackr3* knockdown in trophoblast cells led to a decrease in trophoblast migration. These findings suggest that this decoy receptor may therefore be an important factor in normal placentation.

Keywords

chemokines; decoy receptors; immune cells; and placenta

Address correspondence to: Kathleen M. Caron, 111 Mason Farm Road, 6312B Medical Biomolecular Research Building, CB# 7545, Chapel Hill, North Carolina 27599, USA. Phone: 919.966.5193; kathleen_caron@med.unc.edu.

Author Names:
Kelsey E. Quinn
Brooke C. Matson
Kathleen M. Caron

Introduction

The placenta is a complex yet temporary organ derived from fetal cells that serves as a life-giving and -sustaining force for the developing fetus during pregnancy. The placenta functions as a site of gas and nutrient exchange and is home to specialized immune cell populations that facilitate appropriate placental development and therefore fetal growth. A finite balance of immune cells is critical for the health of a pregnancy, as placental and immune dysfunction is implicated in pregnancy complications such as fetal inflammatory response, preeclampsia, and preterm birth [1]. Uterine natural killer (uNK) cells are the predominant immune cell population found in the placenta during the first trimester of pregnancy, comprising about 70–90% of the total population [2]. uNK cells maintain angiogenic balance through cytokine, chemokine, and angiogenic factor secretion and interact with trophoblast cells to promote trophoblast differentiation and invasion into the spiral arteries [3, 4]. Although still poorly understood, there is a fine-tuned switch of immune cell activation during pregnancy, and overly active uNK and dendritic cells leads to poor placentation and pregnancy complications [5]. Chemokines can help orchestrate the innate immune response during homeostasis and in response to infection, inflammation, and disease [6, 7].

Chemokines bind to canonical signaling receptors as well as to atypical chemokine receptors (ACKRs), which are seven transmembrane G-protein-coupled receptors considered to be “decoy” receptors that favor fine-tuning of chemokine availability through beta-arrestin recruitment rather than typical G-protein-mediated signal transduction. Family members include ACKR1 (formerly DARC), ACKR2 (formerly D6), ACKR3 (formerly CXCR7), and ACKR4 (formerly CCX-CKR or CCRL1). A handful of studies over the past two decades have implicated these receptors in placental development and function [8], not only in humans but also in pigs and sheep [9, 10]. ACKR2 is the decoy receptor best characterized in the placenta to date. ACKR2 is expressed by human trophoblast cells [11], and in cultured primary human trophoblasts, is expressed at a level even higher than classic chemokine receptors [12]. Constitutional deletion of *Ackr2* in mouse dames causes structural defects in the placenta and a higher rate of fetal loss [12].

Less is known about ACKR3 in reproduction. ACKR3 binds the chemokine ligands C-X-C motif chemokine ligand 11 (CXCL11) and 12 (CXCL12), which bind to canonical signaling receptors CXCR3 and CXCR4, respectively. Prior studies have focused on ACKR3 serving as a decoy receptor in the contexts of cardiac and lymphatic development for the endocrine peptide adrenomedullin [13], which also has functional roles in implantation and placentation [14–19].

In the present study, we undertake a comprehensive phenotypic analysis of placentas from *Ackr3*$^{-/-}$ mouse embryos, finding decidual compaction and effects on the population size and spatiotemporal localization of uNK and dendritic cells. We also show that *Ackr3* knockdown in a cultured trophoblast cell line impairs trophoblast migration. These findings implicate *Ackr3* as a mediator of the immune cell environment at the maternal-fetal interface with consequences for trophoblast function and placental vascular development.

Materials and Methods

Mice

3–5 month old heterozygous C57BL/6-*Ackr3*^{tm1Litt}/J-GFP knock-in mice purchased from The Jackson Laboratory (stock #008591). Global constitutive *Ackr3* deletion is embryonic lethal with exception of a small percentage of long-term survivors, therefore, in this study, timed matings were *Ackr3*$^{+/-}$ *x Ackr3*$^{+/-}$ to generate *Ackr3*$^{-/-}$ *and Ackr3*$^{+/+}$ embryos [20]. Females were monitored for vaginal plugs, and the day on which a plug was detected was denoted as embryonic day (e) 0.5. Following euthanasia, placentas were collected at embryonic day (e)12.5-e14.5 of gestation and dissected for further analysis.

Flow Cytometry

Ackr3$^{+/+}$ and *Ackr3*$^{-/-}$ placentas (n=4/per run) from pregnant mice at e12.5 were genotyped by determining GFP signal in each embryo and then minced and enzymatically digested (StemPro Accutase, A1110501) on ice. Each genotype was later validated via PCR. Following tissue dissociation, the samples were incubated at 37°C for 30 min and then passed through a sterile cell strainer to obtain a single-cell suspension. Leukocytes and stromal cells were obtained by density gradient centrifugation (1250 × g, 10 min at 4°C). The cell pellet was then re-suspended with 1 ml RPMI culture medium (Gibco ™, 21875034), and then 500 μl of neat FBS was slowly overlaid above the cell suspension. To pellet viable cells, the suspension was centrifuged for 10 min at 1100 × g at room temperature. The cell pellet was incubated for 30 min. at 4°C with a viability dye (Live/Dead fixable yellow, L34967). The cells were then blocked for non-antigen-specific binding of immunoglobins (CD16/CD32, BD Pharmingen™, 553141) for 10 min., and then antibodies were added (suppl. table 1). Following a 30 min. incubation of antibodies, cells were fixed and then acquired immediately using a Becton Dickinson LSR II and FACSDiva 8.0.1 acquisition software. Results were analyzed using FCS Express 6 (BD Biosciences).

Histology and Immunofluorescence

Placentas were fixed in 4% paraformaldehyde in phosphate buffered saline overnight and then processed into paraffin blocks. Midline cross-sections were cut 5 μm thick. To determine phenotypical differences of the placentas, H and E staining was performed by the UNC Animal Histopathology and Lab Medicine Core and then imaged using a Zeiss Axio Image.A2. For immunofluorescence identification of uterine natural killer (uNK) cells, dendritic (CD11c) cells, and smooth muscle actin (αSMA), placentas were de-paraffinized using a clearing reagent and then rehydrated using a series of ethanol washes. Following antigen retrieval, sections were then blocked with 5% normal donkey serum and incubated overnight at 4°C with the primary antibody CD11c (Proteintech, 17342-1-AP;1:50) or anti-α-Smooth Muscle Actin (Sigma-Aldrich, clone 1A4, A2547; 1:100) and incubated the next day with secondary antibodies including Cy™5 AffiniPure donkey anti-rabbit IgG (Jackson ImmunoResearch; 711-175-152; 1:200), Cy™2 AffiniPure donkey anti-rabbit IgG (Jackson ImmunoResearch; 711-225-152; 1:200), FITC-conjugated DBA lectin (Sigma-Aldrich; L9142; 1:200), and Hoechst (Sigma-Aldrich; B1155; 1:500). Images were acquired using an IX83 Olympus microscope with a Hamamatsu digital camera with cellSens dimension software (Olympus).

Quantitative real time polymerase chain reaction (qPCR)

Placental tissue was snap-frozen in liquid nitrogen and then stored at −80°C until RNA isolation. RNA was extracted using TRIzol Reagent (Invitrogen, Thermo Fisher Scientific) and a Percellys bead homogenizer according to standard procedures and then subsequently treated with DNase1 (RQ1; Promega) and reverse transcribed with M-MLV (Invitrogen, Thermo Fisher Scientific) or iScript (Bio-Rad Laboratories). Quantitative gene expression was assayed with TaqMan® gene expression master mix (Applied Biosystems) and run on a StepOne Plus Real-Time PCR System (Applied Biosystems). Primers and probes for real-time PCR (qPCR) are listed in supplemental table 2. Relative expression levels were determined by the ΔΔCt method and normalized to reference gene expression of *Actb* or *Gapdh*.

Cell culture and RNAi

HTR-8/SVneo (ATCC®CRL-3271) placental trophoblast cells were cultured in RPMI-1640 medium with 5% fetal bovine serum and 1x penicillin/streptomycin and incubated at 37°C containing 5% CO_2. Production of lentiviral particles and infection was performed according to standard protocols by co-transfecting *Ackr3* shRNA pLKO1 vectors (UNC Viral Core) into HEK293T (ATCC®CRL-3216) with lentiviral packaging vectors psPAX2 and MD2.G (Addgene) using Lipofectamine 2000 (ThermoFisher Scientific;11668019) overnight. The following day, collection of viral supernatants via filtration were performed with the addition of 6 ug/ml of polybrene, and HTR-8/SVneo cells were infected for a total of 48 hours before additional assays were performed. Confirmed knockdown was performed via qPCR using *Ackr3* (Applied Biosystems; Hs00664172) and *Actb* (Applied Biosystems; Hs99999903) as housekeeping gene.

Transwell Migration Assay

HTR-8/SVneo cells (6×10^4 cells/well) with *Ackr3* knockdown and empty vector controls were incubated with CellTracker™green CMFDA dye following standardized protocol. Cells were then plated in transwell inserts (Corning; 354578) and incubated overnight. The transwell inserts were then fixed in 4% paraformaldehyde in phosphate buffered saline for 20 min. and then each filter was removed and mounted onto glass slides for fluorescent imaging. The percentage area coverage was analyzed using Fiji [21].

Statistical Analysis

Data presented was analyzed as mean + SEM unless otherwise noted. All statistics were performed in GraphPad Prism 5 (version 5.01). For flow cytometry, immune cell analysis was calculated as a percentage of gated cells and analyzed using an unpaired t-test with Welch's correction. The space/area left in each transwell was calculated to assess overall migration and cell coverage using Fiji [21]. Overall trophoblast migration was determined using an unpaired two-tailed t-test with Welch's correction. Fetal sinus area was measured using the trace tool in Fiji and the total area measurement was calculated using an unpaired t-test with Welch's correction.

Results

Embryonic Deletion or Knockdown of *Ackr3* augments trophoblast migration and fetal sinuses

With previous research reporting ACKR3 expression in trophoblast and endothelial cells of the placenta, we aimed to investigate further the significance of ACKR3 during placentation [22, 23]. First, we completed a comprehensive morphometric analysis of e14.5 placentas from *Ackr3*$^{+/+}$ and *Ackr3*$^{-/-}$ embryos. The gross pathology of placentas of *Ackr3*$^{+/+}$ and *Ackr3*$^{-/-}$ embryos at e14.5 was similar without changes in labyrinth height or length (Figure 1a). Upon further histological evaluation of the labyrinth, we observed an increase in spacing in between the fetal and maternal sinuses in placentas of *Ackr3*$^{-/-}$ embryos, leading to an increase in fetal sinus area (Figure 1b). Additionally, clusters of syncytial trophoblast cells in the labyrinth appeared to be reduced in placentas of *Ackr3*$^{-/-}$ embryos (Figure 1b). Due to the reduction in trophoblast outgrowth to the labyrinth in placentas of *Ackr3*$^{-/-}$ embryos, we next wanted to determine if *in vitro* loss of *Ackr3* could affect trophoblast cell migration. Using an *in vitro* transwell assay, we demonstrated that knockdown of *Ackr3* in HTR8/Svneos caused a decrease in trophoblast migration compared to negative controls (Figure 1c).

Embryonic deletion of *Ackr3* increases immune cell populations in the decidua

Because immune and trophoblast cells can cooperatively regulate placental development, we next wanted to determine if deletion of *Ackr3* could affect placental development at an earlier time point. In the mouse placenta, heavy immune cell recruitment and trophoblast migration occurs between e11.5–12.5, enabling growth and formation of the placenta and increasing blood flow at the fetal-maternal interface. We first analyzed placental morphology at e12.5 in *Ackr3*$^{-/-}$ embryos compared to *Ackr3*$^{+/+}$ counterparts. At initial glance, placentas from *Ackr3*$^{-/-}$ embryos appeared to be no different from *Ackr3*$^{+/+}$ placentas (Figure 2a). However, further evaluation demonstrated that embryonic deletion of *Ackr3* at e12.5 caused a slightly more dense and compacted decidua compared to *Ackr3*$^{+/+}$ littermates (Figure 2b). Because this compaction could be due to changes in immune cells and cytokine secretion in the decidua, we next measured cytokine and chemokine expression in e11.5 placentas. C-X-C motif chemokine ligand 10 (Cxcl10) gene expression decreased in placentas from *Ackr3*$^{-/-}$ embryos, but there was no other difference in cytokine or chemokine expression between placentas of *Ackr3*$^{+/+}$ and *Ackr3*$^{-/-}$embryos (Figure 2c). It is important to note that mice on the B6 background lack a functional *Cxcl11* gene; therefore, we did not evaluate *Cxcl11* expression in this study [24].

We next utilized flow cytometry to broadly quantify common immune cell populations in the placenta at e12.5. Uterine natural killer (uNK) and dendritic (DC) cells increased significantly in *Ackr3*$^{-/-}$ placentas, whereas macrophages had a tendency to increase (Figure 3a). To confirm the increase in uNK and dendritic cells in *Ackr3*$^{-/-}$ placentas, we next stained for uNKs and DCs via immunofluorescence. Consistent with flow cytometry data, we again observed an increase in uNKs and DC cells in *Ackr3*$^{-/-}$ placentas compared to wildtype counterparts (Figure 3b). Interestingly, in *Ackr3*$^{-/-}$ placentas, we observed less

frequent co-localization of uNK cell and DC populations, which could alter normal uNK and DC crosstalk needed during pregnancy [25, 26].

Embryonic *Ackr3* is not required for spiral artery remodeling

To determine whether our observed increase in uNK cell and DC populations in placentas of *Ackr3*$^{-/-}$ embryos could affect placental development, we next wanted to evaluate if there was a change in spiral artery remodeling. During early pregnancy, spiral arteries transition from thick to thin-walled arteries, characterized by a loss in smooth muscle coverage and an increase in luminal area, to allow optimal flow of oxygenated blood to the growing embryo. Immune cells, specifically uNK cells, have been shown to play a role in the spiral artery remodeling process [27]. The quantitative measurement of spiral arteries in placentas of *Ackr3*$^{+/+}$ and *Ackr3*$^{-/-}$ embryos revealed similar luminal and relative wall areas (Figure 4a). We also did not observe a difference in smooth muscle actin, which is expressed by vascular smooth muscle cells, and used as an indicator for spiral artery remodeling (Figure 4b).

Discussion

Changes in the proportions of immune cell population subsets, including increases in innate immune cell populations are parts of normal pregnancy physiology [28]. Increases in immune cells such as macrophages and uNK cells facilitate proper trophoblast migration and spiral artery remodeling in the placenta in support of fetal growth and development [29, 30]. Several pregnancy complications, such as, preeclampsia, fetal growth restriction, and preterm birth, among others, have been associated with alterations in immune cell populations in the placental bed. Therefore, further understanding of immune cell population dynamics is critically important for characterizing placental development, understanding the pathophysiology of these pregnancy complications, and developing potential prophylactic and therapeutic interventions [4, 28].

Due to its non-canonical signaling attributes, few studies have investigated the role of ACKR3 during pregnancy and specifically how it regulates placentation [31, 32]. Here, we have phenotypically characterized placentas from *Ackr3*$^{-/-}$ mouse embryos during the timeframe of immune cell recruitment, trophoblast invasion, and spiral artery remodeling. Tightly controlled chemokine and cytokine activity is important for eliciting proper immune responses [33, 34]. The increase in uNK and dendritic cells of placentas from *Ackr3*$^{-/-}$ embryos may be due to the absence of ACKR3 scavenger activity, therefore changing the cytokine and chemokine dynamic in immune response.

In association with an increase in uNK and dendritic cells, we also observed a decrease in trophoblast migration and an increase in fetal sinus area in placentas of *Ackr3*$^{-/-}$ embryos. As mentioned, uNK cells can regulate the invasion of trophoblast cells in the placenta through production of growth factors and cytokines such as VEGF and tumor necrosis factor (TNF). However, over production of uNK cells could cause an abnormal cytotoxic response leading to trophoblast apoptosis or inhibiting efficient trophoblast invasion [35]. Notably, in this study, the observed changes in trophoblast invasion and poor fetal sinus development leads us to believe that ACKR3 primarily attributes to proper trophoblast invasion in the placenta either through regulating immune cell populations or ligand concentrations at the

fetal-maternal interface. Indeed, others have also identified that ACKR3 protein expression was lower in trophoblast cells from pregnancies complicated by preeclampsia [36].

We surprisingly observed a decrease in *Cxcl10* in placentas of *Ackr3*$^{-/-}$ embryos. Because uNK cells express CXCR3, the receptor for CXCL10, an increase in uNK cells in *Ackr3*$^{-/-}$ embryos could possibly cause an overexpression of CXCR3 on the surface of uNK cells, and lead to receptor desensitization.

From this study, we can conclude that ACKR3 contributes to immune cell population dynamics in the placenta. Because ACKR3 signals primarily through β-arrestin-mediated signaling, future studies will identify downstream mechanisms of ACKR3 in response to the ligands, CXCL11, CXCL12, and adrenomedullin [37, 38]. Nevertheless, ACKR3 roles in immune cell recruitment identified in this study will provide future research into precursors or targets for immune cell-mediated pregnancy disorders.

Supplementary Material

Refer to Web version on PubMed Central for supplementary material.

Acknowledgements

The authors acknowledge the University of North Carolina at Chapel Hill Animal Histopathology Core, the UNC Flow Cytometry Core Facility (supported in part by P30 CA016086 Cancer Center Core Support Grant to the UNC Lineberger Comprehensive Cancer Center), and previous Caron laboratory members, Scott T. Espenschied, Stephanie L. Pierce, and Dan O. Kechele for their assistance and guidance in prepping samples. This work was supported by the National Institutes of Health to KMC [RO1 HD060860] and The Lalor Foundation Fellowship to KEQ.

Glossary

Ackr3	Atypical chemokine receptor 3
AM	adrenomedullin
uNK	uterine natural killer cells
DC	dendritic cells

References

1. Yang F, Zheng Q, Jin L: Dynamic Function and Composition Changes of Immune Cells During Normal and Pathological Pregnancy at the Maternal-Fetal Interface. Front Immunol 2019, 10:2317. [PubMed: 31681264]
2. Fukui A, Funamizu A, Yokota M, Yamada K, Nakamua R, Fukuhara R, Kimura H, Mizunuma H: Uterine and circulating natural killer cells and their roles in women with recurrent pregnancy loss, implantation failure and preeclampsia. J Reprod Immunol 2011, 90(1):105–110. [PubMed: 21632120]
3. Dosiou C, Giudice LC: Natural killer cells in pregnancy and recurrent pregnancy loss: endocrine and immunologic perspectives. Endocr Rev 2005, 26(1):44–62. [PubMed: 15689572]
4. LaMarca BD, Ryan MJ, Gilbert JS, Murphy SR, Granger JP: Inflammatory cytokines in the pathophysiology of hypertension during preeclampsia. Curr Hypertens Rep 2007, 9(6):480–485. [PubMed: 18367011]

5. Pollheimer J, Vondra S, Baltayeva J, Beristain AG, Knofler M: Regulation of Placental Extravillous Trophoblasts by the Maternal Uterine Environment. Front Immunol 2018, 9:2597. [PubMed: 30483261]
6. Griffith JW, Sokol CL, Luster AD: Chemokines and chemokine receptors: positioning cells for host defense and immunity. Annu Rev Immunol 2014, 32:659–702. [PubMed: 24655300]
7. Sokol CL, Luster AD: The chemokine system in innate immunity. Cold Spring Harb Perspect Biol 2015, 7(5).
8. Borroni EM, Bonecchi R, Buracchi C, Savino B, Mantovani A, Locati M: Chemokine decoy receptors: new players in reproductive immunology. Immunol Invest 2008, 37(5):483–497. [PubMed: 18716935]
9. Quinn KE, Prosser SZ, Kane KK, Ashley RL: Inhibition of chemokine (C-X-C motif) receptor four (CXCR4) at the fetal-maternal interface during early gestation in sheep: alterations in expression of chemokines, angiogenic factors and their receptors. J Anim Sci 2017, 95(3):1144–11153. [PubMed: 28380526]
10. Wessels JM, Linton NF, van den Heuvel MJ, Cnossen SA, Edwards AK, Croy BA, Tayade C: Expression of chemokine decoy receptors and their ligands at the porcine maternal-fetal interface. Immunol Cell Biol 2011, 89(2):304–313. [PubMed: 20680026]
11. Martinez de la Torre Y, Buracchi C, Borroni EM, Dupor J, Bonecchi R, Nebuloni M, Pasqualini F, Doni A, Lauri E, Agostinis C et al.: Protection against inflammation- and autoantibody-caused fetal loss by the chemokine decoy receptor D6. Proc Natl Acad Sci U S A 2007, 104(7):2319–2324. [PubMed: 17283337]
12. Teoh PJ, Menzies FM, Hansell CAH, Clarke M, Waddell C, Burton GJ, Nelson SM, Nibbs RJB: Atypical chemokine receptor ACKR2 mediates chemokine scavenging by primary human trophoblasts and can regulate fetal growth, placental structure, and neonatal mortality in mice. J Immunol 2014, 193(10):5218–5228. [PubMed: 25297873]
13. Klein KR, Karpinich NO, Espenschied ST, Willcockson HH, Dunworth WP, Hoopes SL, Kushner EJ, Bautch VL, Caron KM: Decoy receptor CXCR7 modulates adrenomedullin-mediated cardiac and lymphatic vascular development. Dev Cell 2014, 30(5):528–540. [PubMed: 25203207]
14. Li M, Schwerbrock NMJ, Lenhart PM, Fritz-Six KL, Kadmiel M, Christine KS, Kraus DM, Espenschied ST, Willcockson HH, Mack CP et al.: Fetal-derived adrenomedullin mediates the innate immune milieu of the placenta. J Clin Invest 2013, 123(6):2408–2420. [PubMed: 23635772]
15. Li M, Wu Y, Caron KM: Haploinsufficiency for adrenomedullin reduces pinopodes and diminishes uterine receptivity in mice. Biology of reproduction 2008, 79(6):1169–1175. [PubMed: 18716289]
16. Li M, Yee D, Magnuson TR, Smithies O, Caron KM: Reduced maternal expression of adrenomedullin disrupts fertility, placentation, and fetal growth in mice. J Clin Invest 2006, 116(10):2653–2662. [PubMed: 16981008]
17. Matson BC, Caron KM: Adrenomedullin and endocrine control of immune cells during pregnancy. Cell Mol Immunol 2014, 11(5):456–459. [PubMed: 25132453]
18. Matson BC, Corty RW, Karpinich NO, Murtha AP, Valdar W, Grotegut CA, Caron KM: Midregional pro-adrenomedullin plasma concentrations are blunted in severe preeclampsia. Placenta 2014, 35(9):780–783. [PubMed: 25043691]
19. Matson BC, Pierce SL, Espenschied ST, Holle E, Sweatt IH, Davis ES, Tarran R, Young SL, Kohout TA, van Duin M et al.: Adrenomedullin improves fertility and promotes pinopodes and cell junctions in the peri-implantation endometrium. Biol Reprod 2017, 97(3):466–477. [PubMed: 29025060]
20. Cruz-Orengo L, Holman DW, Dorsey D, Zhou L, Zhang P, Wright M, McCandless EE, Patel JR, Luker GD, Littman DR et al.: CXCR7 influences leukocyte entry into the CNS parenchyma by controlling abluminal CXCL12 abundance during autoimmunity. J Exp Med 2011, 208(2):327–339. [PubMed: 21300915]
21. Schindelin J, Arganda-Carreras I, Frise E, Kaynig V, Longair M, Pietzsch T, Preibisch S, Rueden C, Saalfeld S, Schmid B et al.: Fiji: an open-source platform for biological-image analysis. Nat Methods 2012, 9(7):676–682. [PubMed: 22743772]

22. Berahovich RD, Zabel BA, Lewen S, Walters MJ, Ebsworth K, Wang Y, Jaen JC, Schall TJ: Endothelial expression of CXCR7 and the regulation of systemic CXCL12 levels. Immunology 2014, 141(1):111–122. [PubMed: 24116850]

23. Liu Y, Fan X, Wang R, Lu X, Dang YL, Wang H, Lin HY, Zhu C, Ge H, Cross JC et al.: Single-cell RNA-seq reveals the diversity of trophoblast subtypes and patterns of differentiation in the human placenta. Cell Res 2018, 28(8):819–832. [PubMed: 30042384]

24. Sierro F, Biben C, Martinez-Munoz L, Mellado M, Ransohoff RM, Li M, Woehl B, Leung H, Groom J, Batten M et al.: Disrupted cardiac development but normal hematopoiesis in mice deficient in the second CXCL12/SDF-1 receptor, CXCR7. Proceedings of the National Academy of Sciences of the United States of America 2007, 104(37):14759–14764. [PubMed: 17804806]

25. Blois SM, Barrientos G, Garcia MG, Orsal AS, Tometten M, Cordo-Russo RI, Klapp BF, Santoni A, Fernandez N, Terness P et al.: Interaction between dendritic cells and natural killer cells during pregnancy in mice. J Mol Med (Berl) 2008, 86(7):837–852. [PubMed: 18506412]

26. Walzer T, Dalod M, Vivier E, Zitvogel L: Natural killer cell-dendritic cell crosstalk in the initiation of immune responses. Expert Opin Biol Ther 2005, 5 Suppl 1:S49–59. [PubMed: 16187940]

27. Ashkar AA, Di Santo JP, Croy BA: Interferon gamma contributes to initiation of uterine vascular modification, decidual integrity, and uterine natural killer cell maturation during normal murine pregnancy. J Exp Med 2000, 192(2):259–270. [PubMed: 10899912]

28. Cornelius DC, Cottrell J, Amaral LM, LaMarca B: Inflammatory mediators: a causal link to hypertension during preeclampsia. Br J Pharmacol 2019, 176(12):1914–1921. [PubMed: 30095157]

29. Cornelius DC: Preeclampsia: From Inflammation to Immunoregulation. Clin Med Insights Blood Disord 2018, 11:1179545X17752325.

30. Cornelius DC, Wallace K: Decidual natural killer cells: A critical pregnancy mediator altered in preeclampsia. EBioMedicine 2019, 39:31–32. [PubMed: 30594551]

31. Han J, Yoo I, Lee S, Jung W, Kim HJ, Hyun SH, Lee E, Ka H: Atypical chemokine receptors 1, 2, 3 and 4: Expression and regulation in the endometrium during the estrous cycle and pregnancy and with somatic cell nucleus transfer-cloned embryos in pigs. Theriogenology 2019, 129:121–129. [PubMed: 30844653]

32. Lim W, Bae H, Bazer FW, Song G: Cell-specific expression and signal transduction of C-C motif chemokine ligand 2 and atypical chemokine receptors in the porcine endometrium during early pregnancy. Dev Comp Immunol 2018, 81:312–323. [PubMed: 29278679]

33. Bonecchi R, Garlanda C, Mantovani A, Riva F: Cytokine decoy and scavenger receptors as key regulators of immunity and inflammation. Cytokine 2016, 87:37–45. [PubMed: 27498604]

34. Bonecchi R, Graham GJ: Atypical Chemokine Receptors and Their Roles in the Resolution of the Inflammatory Response. Front Immunol 2016, 7:224. [PubMed: 27375622]

35. Yougbare I, Tai WS, Zdravic D, Oswald BE, Lang S, Zhu G, Leong-Poi H, Qu D, Yu L, Dunk C et al.: Activated NK cells cause placental dysfunction and miscarriages in fetal alloimmune thrombocytopenia. Nat Commun 2017, 8(1):224. [PubMed: 28794456]

36. Lu J, Zhou WH, Ren L, Zhang YZ: CXCR4, CXCR7, and CXCL12 are associated with trophoblastic cells apoptosis and linked to pathophysiology of severe preeclampsia. Exp Mol Pathol 2016, 100(1):184–191. [PubMed: 26721717]

37. Benredjem B, Girard M, Rhainds D, St-Onge G, Heveker N: Mutational Analysis of Atypical Chemokine Receptor 3 (ACKR3/CXCR7) Interaction with Its Chemokine Ligands CXCL11 and CXCL12. J Biol Chem 2017, 292(1):31–42. [PubMed: 27875312]

38. Mackie DI, Nielsen NR, Harris M, Singh S, Davis RB, Dy D, Ladds G, Caron KM: RAMP3 determines rapid recycling of atypical chemokine receptor-3 for guided angiogenesis. Proc Natl Acad Sci U S A 2019, 116(48):24093–24099. [PubMed: 31712427]

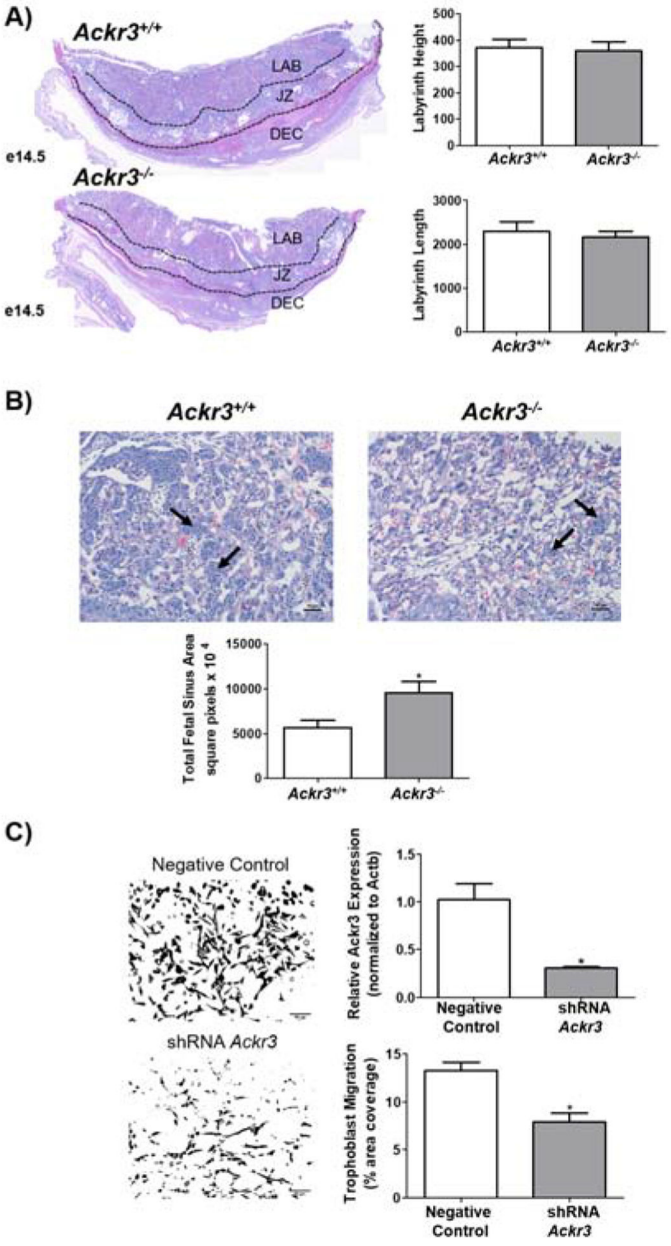

Figure 1.

(A) The placental morphology, labyrinth height, and labyrinth length in placentas of *Ackr3*$^{-/-}$ embryos is similar to *Ackr3*$^{+/+}$ at e14.5 (per genotype, $n = 6–7$ total placentas, unpaired t-test with Welch's correction). **(B)** A decrease in clusters of trophoblast cells (arrows) and an increase in fetal sinus area are observed in labyrinth of *Ackr3*$^{-/-}$ embryos compared to *Ackr3*$^{+/+}$ at e14.5 (per genotype, $n = 6–7$ total placentas, unpaired t-test with Welch's correction). **(C)** Reduction of *Ackr3* in extravillous trophoblast cells (HTR8/svNeos) *in vitro* causes a decrease in trophoblast migration. Scale bars: 50 μm. The space/area left in each transwell was calculated to assess overall migration and cell coverage using Fiji. Overall trophoblast migration was determined using an unpaired two-tailed t-test with Welch's correction. $*P < 0.05$.

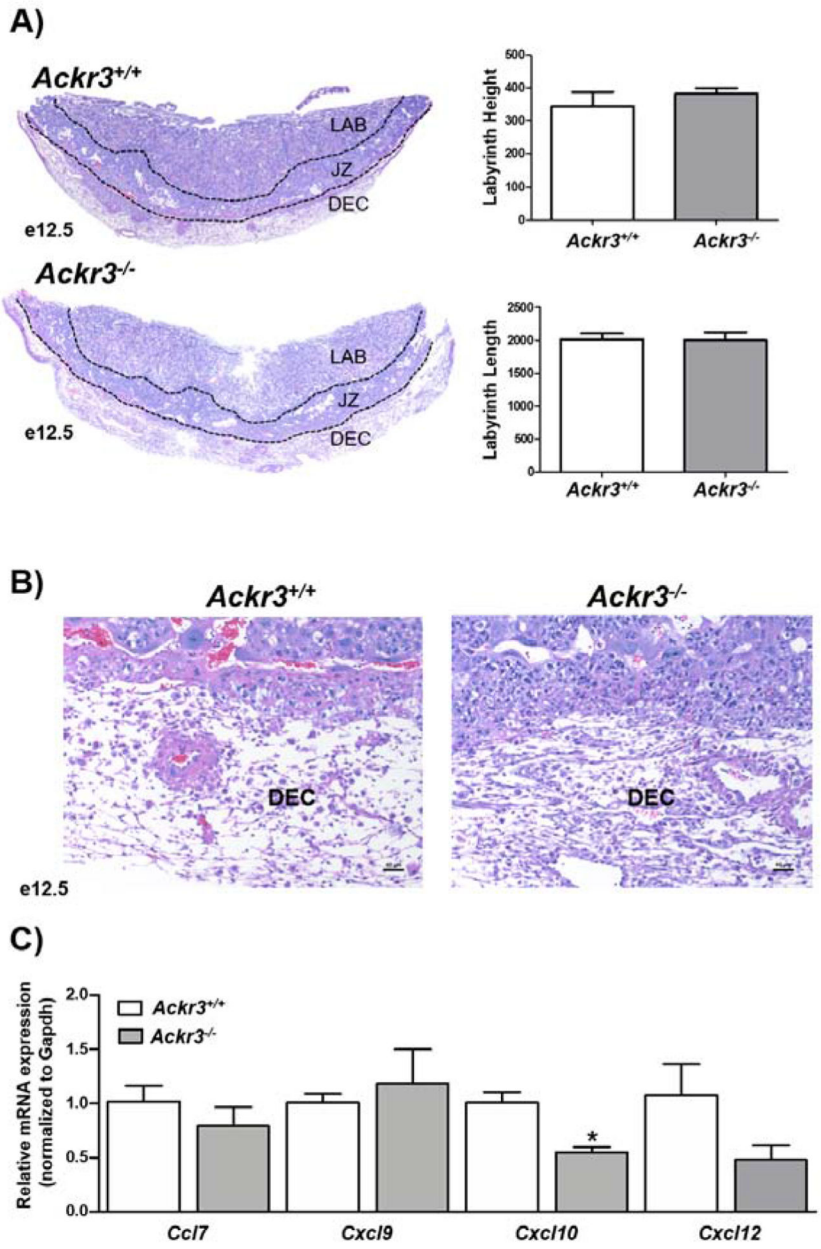

Figure 2.

(A) The placental morphology, labyrinth height and labyrinth length in placentas of *Ackr3*$^{-/-}$ embryos is similar to *Ackr3*$^{+/+}$ at e12.5 (per genotype, $n = 5–6$ total placentas, unpaired t-test with Welch's correction). **(B)** Embryonic deletion of *Ackr3* at e12.5 causes an increase in cellular density in the decidua (DEC) compared to wildtype controls. Scale bar, 40 μm. **(C)** *Cxcl10* gene expression decreases in e12.5 placentas of *Ackr3*$^{-/-}$ embryos compared to *Ackr3*$^{+/+}$ embryos. Gene expression of additional cytokines is similar in e12.5 placentas of *Ackr3*$^{+/+}$ and *Ackr3*$^{-/-}$ embryos. Data graphed as $2^{-\Delta\Delta CT}$ with mean ± SEM. $^{*}P < 0.05$.

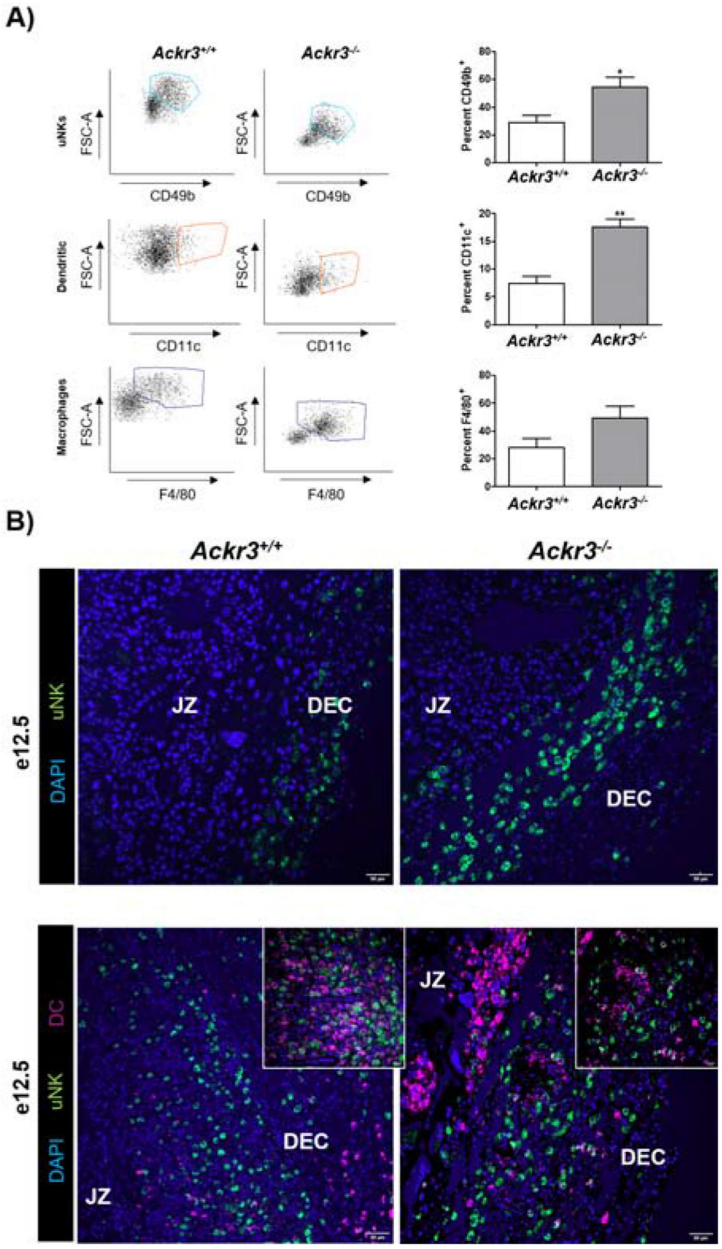

Figure 3.

(A) Flow cytometry of e12.5 placentas in *Ackr3*$^{+/+}$ and *Ackr3*$^{-/-}$ embryos. Placentas from *Ackr3*$^{-/-}$ embryos have an increase in uterine natural killer (uNK), and dendritic cells, and a trending increase of macrophages. Immune cell analysis was calculated as a percentage of gated cells and analyzed using an unpaired t-test with Welch's correction. **P*<0.05, ***P*<0.01. **(B)** Uterine natural killer (uNK) cells (denoted in green) increase in e12.5 placentas of *Ackr3*$^{-/-}$ embryos compared to wildtype counterparts (left panel). Co-localization of dendritic cells (CD11c, denoted in magenta) and uNK cells decrease in embryos null of *Ackr3* (right panel). Scale bars: 50 μm. Decidua, DEC, junctional zone, JZ.

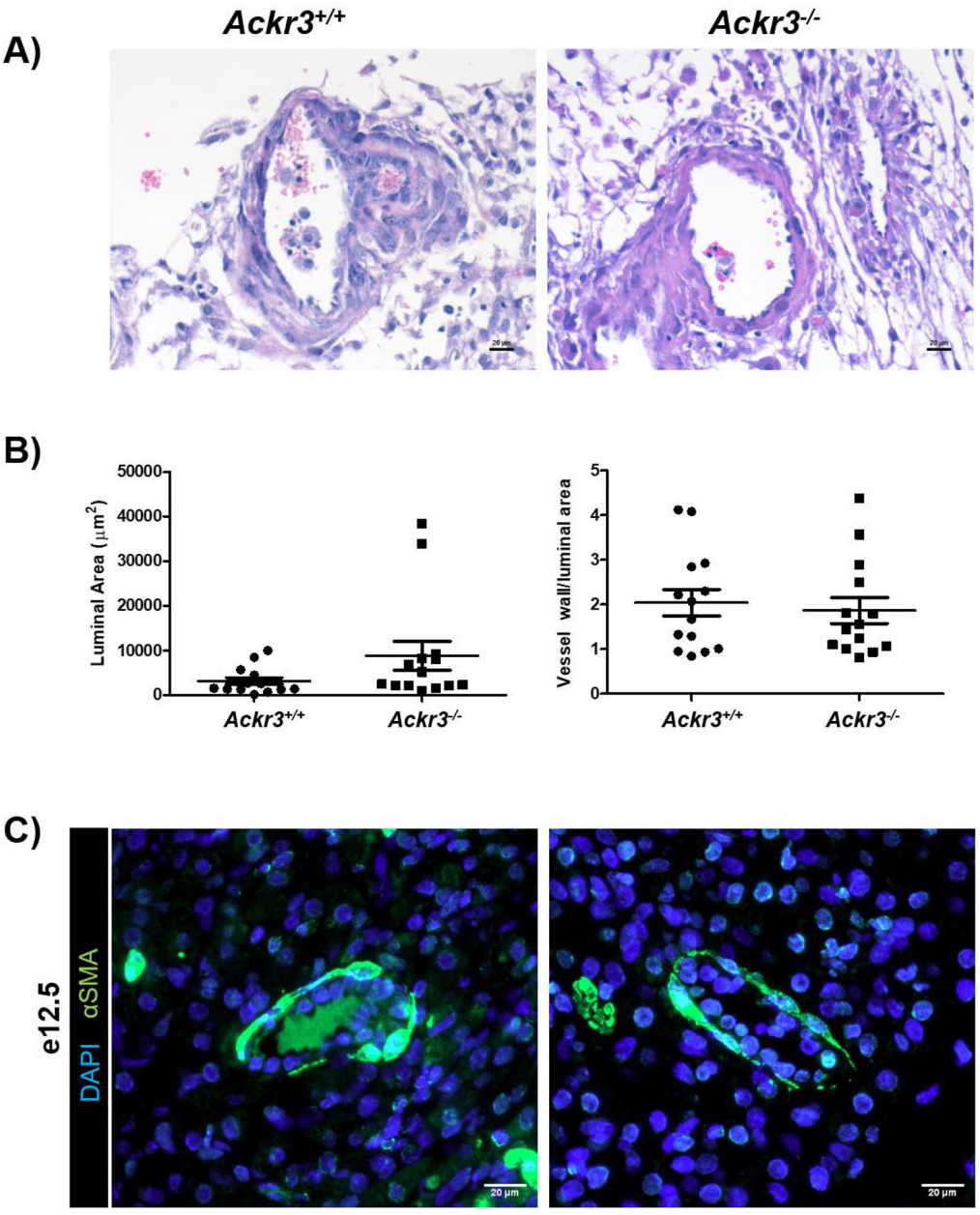

Figure 4.

(A) H&E staining of spiral arteries in *Ackr3*$^{+/+}$ and *Ackr3*$^{-/-}$ embryos at e12.5 (per genotype, n = 5–6 total placentas, unpaired t-test with Welch's correction). **(B)** Quantification of the luminal area and wall thickness (ratio of vessel wall to lumen area) of spiral arteries in *Ackr3*$^{+/+}$ and *Ackr3*$^{-/-}$ embryos at e12.5. **(C)** At e12.5 smooth muscle coverage (αSMA, green) is similar between *Ackr3*$^{+/+}$ and *Ackr3*$^{-/-}$ embryos (per genotype, n = 5–6 total placentas).